Chapter 1

Introduction: Galactic High–Latitude Molecular Clouds

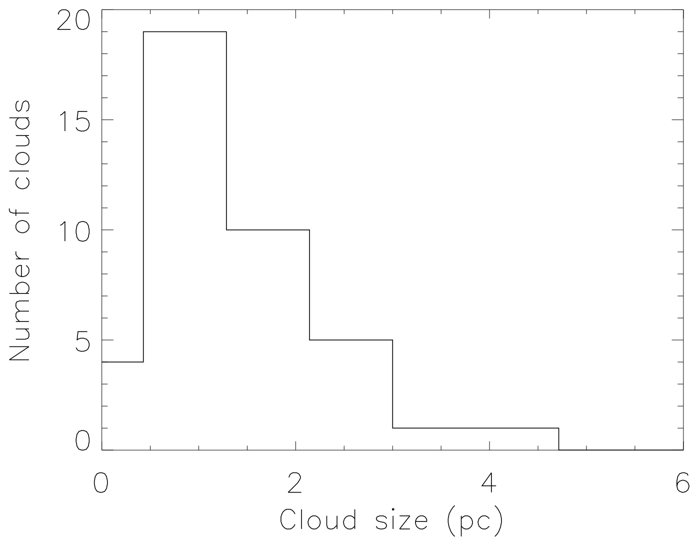

Fig. 1.1.— The size distribution of Milky Way molecular clouds located at high ($|b| \geq 25°$) Galactic latitudes. High–latitude clouds contribute only 20% of the local molecular mass (Magnani *et al.* 1996), but this understates the importance of these objects. As isolated translucent clouds they probe the transition from atomic to molecular gas, which occurs on the surface of *all* molecular clouds.

1.1 The Distribution of Interstellar Matter

> The problem of the masses of the dark nebulae is fraught with difficulty, and we do not venture to suggest any conclusion. *Eddington (1926)*

How much matter is in between the stars, and what are its properties? Struve (1941) used an analogy: the stars in the Galaxy are like raindrops, separated from each other by an average distance of 40 miles. Nearly all of the space between these stars consists of gas which is extremely rarefied: a hot ($T \sim 10^6$ K) ionized medium with density $n \sim 0.005\,\mathrm{cm}^{-3}$, which produces X-rays, and a warm ($T \sim 8000$ K) "intercloud medium" with density $n \sim 0.3\,\mathrm{cm}^{-3}$, which produces H$\alpha$ emission. These components each occupy nearly 50% of the volume. Half of the gas mass in the Galaxy, however, is in the form of giant molecular clouds (GMCs), which occupy less than 1% of the volume. Matter is continually cycled between the low and high density phases, and each phase is directly related to a different stage in stellar evolution: the rarefied gas is produced by supernova explosions and by stellar winds, while the GMCs, as well as smaller dark molecular clouds, are the primary sites of star formation.

1.1.1 The Local Interstellar Environment

If the Solar neighborhood is a typical region of the Galaxy, then much can be learned about the average interstellar environment by studying the local interstellar medium (ISM). The Sun, as well as many of the most familiar naked-eye stars, is located within the Local Hot Bubble (LHB), an irregularly shaped cavity which is filled with highly rarefied 10^6 K gas, an example of the hot ionized component mentioned above. The cavity varies from 40 to 130 pc in radial extent from the Sun (Snowden *et al.* 1998). Figure 2 shows the morphology of the LHB, as determined from $\frac{1}{4}$ keV X-ray data by

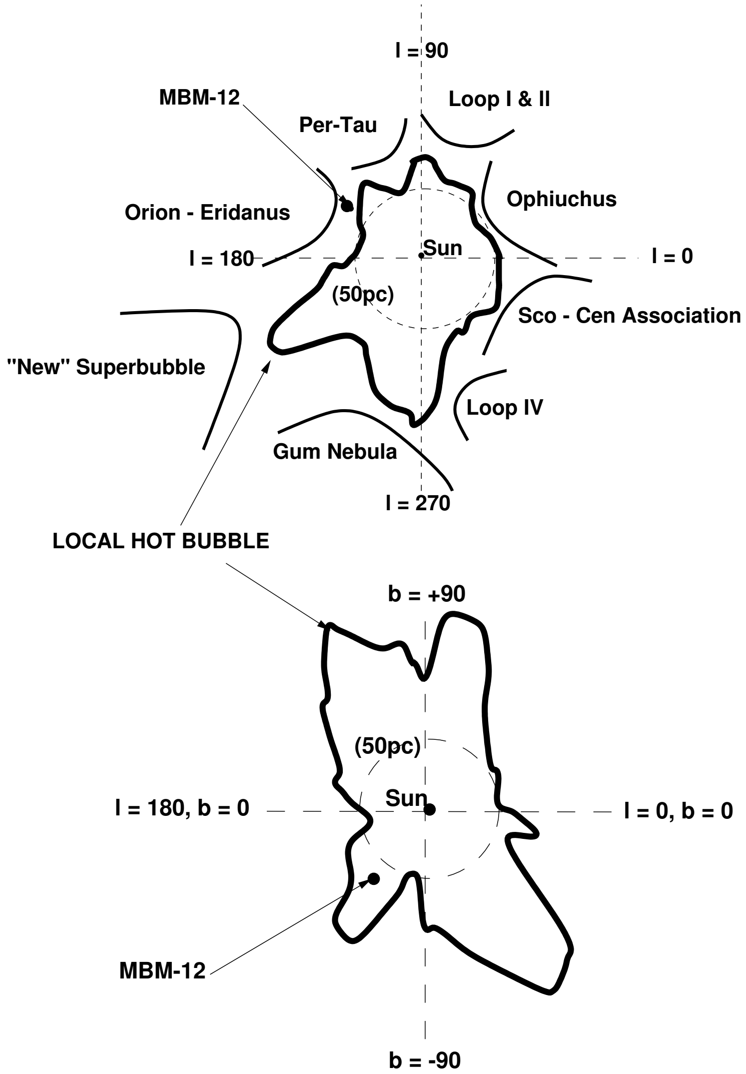

Fig. 1.2.— The Local Hot Bubble (LHB). The thick solid line marks the approximate extent of the LHB as determined from X-ray data (Snowden *et al.* 1998). The approximate location of high-latitude cloud MBM-12 is indicated. (Top) A view from the North Galactic Pole. Adjacent bubbles and shell structures are indicated schematically (after Welsh *et al.* 1994). The approximate position of the edge of the "New Superbubble" discovered by Heiles (1998) is also drawn. (Bottom) A view in the Galactic plane, along an axis from $\ell = 270\,^\circ$ to $\ell = 90\,^\circ$.

Snowden *et al.* (1998). The locations of nearby bubbles and shell-like structures are shown schematically (*cf.*, Welsh, Craig, Vedder, & Vallerga 1994; Heiles 1998).

The LHB is believed to be an expanding shell produced either by a nearby supernova explosion or by the stellar winds of an OB association. Similar events occur throughout the Galaxy (as well as in other galaxies). When adjacent expanding bubbles meet, the gas is compressed, and 21 cm H I emission is observed in the interface regions between bubbles. The temperature of this gas is of order 100 K (Kulkarni & Heiles 1987): the compressed ionized gas has recombined and cooled. This "inter-bubble" gas is a part of the cold neutral medium (CNM) which accounts for approximately 40% of the gas mass in the Galaxy.

1.1.2 The High Galactic Latitude Molecular Clouds

Not all of the molecular mass in the Galaxy resides in GMCs and dark clouds. The nearest molecular clouds are the high Galactic latitude molecular clouds (HLCs), first defined as a class by Magnani, Blitz, & Mundy (1985, hereafter MBM). Over 100 molecular clouds with latitudes $|b|\gtrsim 25^\circ$ have been detected in CO emission to date (see the catalog of Magnani, Hartmann, & Speck 1996). Many of these clouds have had their distances constrained using the presence or absence of sodium, deuterium, and calcium absorption towards stars along lines of sight towards the clouds (e.g., see Hobbs, Blitz, & Magnani 1986; Hobbs *et al.* 1988; Welty *et al.* 1989). A photometric method was also used to estimate the distances to some HLCs (Penprase 1992). The average distance to the ~ 40 clouds with measured distances is 105 pc (Magnani *et al.* 1996). These clouds must therefore lie either inside the Local Hot Bubble, or on its edges. The average conditions in the LHB are not conducive to molecule formation, so it is probable that the HLCs are the molecular component of the compressed cold gas at the interface between the LHB and adjacent bubbles. Indeed, the nearest molecular cloud, high–latitude cloud MBM-12, seems to be at the edge of the LHB (Kuntz, Snowden, & Verter 1997; also see Chapter 3), and is even used to calibrate the size of the Bubble (Snowden *et al.* 1998). Figure 2 shows the approximate location of MBM-12.

The HLCs are Galactic plane objects: the rms scale height of these clouds is $h \approx 87\,\mathrm{pc}$ (Magnani *et al.* 1996). If the Solar neighborhood is not unusual, then clouds like the HLCs exist throughout the Galaxy. The HLCs are low–extinction clouds which were first identified by visual inspection of the Palomar Observatory Sky Survey (POSS) plates (MBM; Keto & Myers 1986). Such clouds can only be observed nearby, and were searched for at high latitudes to avoid confusion with the more distant high-extinction sources in the Galactic plane. Most of the HLCs have modest visual extinctions, $\mathrm{A_v} \approx 1-5$ magnitudes; as such they exist in the *translucent* photochemical regime (van Dishoeck & Black 1988; see below).

For the 41 clouds with known distance, the cloud size, R, can be estimated. Table 2 of Magnani *et al.* (1996) lists distance, d, and cloud area, Ω, for their catalog sources. The value Ω is a solid angle determined from CO maps of the clouds. The linear size may be determined from $R \approx d\sqrt{\Omega}$. Most of the source listings in Magnani *et al.* (1996) give a range of distances, bracketed using stellar absorption measurements. For those objects, d was assumed to be the average of the two distances.

The distribution of HLC sizes is plotted in Figure 1. Half of the clouds have sizes between 0.5 and 1.25 pc. The HLCs are much smaller than the low–latitude GMCs and dark clouds, which have sizes of order $10 - 100$ pc. The nearest molecular cloud, HLC MBM-12, has a size of ~ 2 pc, larger than the typical HLCs.

1.1.3 The Translucent Interstellar Medium

> Observation of a molecule in the interstellar gas reflects the end result of an often delicate balance between formation and destruction.
>
> *Duley & Williams (1984)*

Translucent clouds are clouds with visual extinctions spanning the range $A_v \approx 1 - 5$ which are exposed to the average interstellar far-ultraviolet (FUV) ($6\,\mathrm{eV} < h\nu < 13.6\,\mathrm{eV}$) radiation field. In their pioneering work on CO photodissociation in the interstellar medium, van Dishoeck & Black (1988) introduced the class of translucent clouds as intermediate objects between the low-extinction diffuse clouds, which contain few molecules, and the optically thick dark molecular clouds, whose interiors are entirely free of FUV photons. Photodestruction plays an important role in the chemistry of translucent clouds, as it does in diffuse H I clouds; at the same time translucent clouds are primarily molecular, as are dark clouds. Translucent clouds are therefore the simplest kind of molecular cloud in which CO is observable. There is growing observational evidence which shows that much of the molecular gas mass in the Galaxy is translucent (Polk *et al.* 1988; Wright *et al.* 1992; Chiar *et al.* 1994). Therefore the study of translucent clouds can answer many questions regarding molecule formation in the general molecular environment. High–latitude clouds contribute only 20% of the local molecular mass (Magnani *et al.* 1996), but this understates the importance of these objects. As isolated translucent clouds they probe the transition from atomic to molecular gas, which occurs on the surface of *all* molecular clouds without internal UV sources.

1.1.4 Tracing translucent H_2: Carbon Gas

Hydrogen is the most abundant element in the Universe. The most stable form of hydrogen at low temperatures is the hydrogen molecule H_2. Therefore, in cold, well-shielded regions of interstellar space, H_2 should be the most abundant chemical species (Field, Somerville, & Dressler 1966). Unfortunately, H_2 is a symmetric molecule, with no permanent electric dipole moment. It cannot be observed in emission in cold interstellar clouds. The most abundant chemically active elements after hydrogen are oxygen and carbon, thus the carbon monoxide (CO) molecule is expected to be the most abundant molecule after H_2. Since CO has a small permanent electric dipole moment ($\mu = 0.112$ debye), its lowest rotational energy levels are easily excited into emission by collisions. Consequently, CO transitions are typically used to probe the distribution of and physical conditions in H_2 gas.

Unfortunately, CO is not expected to exist *everywhere* that H_2 exists. The balance between formation and destruction proceeds differently for H_2 than for CO. While both species are shielded from the FUV radiation field equally by dust grains, H_2 and CO molecules also *self–shield*. Dissociation of H_2 occurs by absorption of UV photons in the Lyman and Werner bands, and subsequent fluorescence to a continuum state (Federman, Glassgold, & Kwan 1979; van Dishoeck & Black 1986). For high enough column density of H_2, the transitions saturate. As a result, photons capable of dissociating H_2 will penetrate no further than a certain depth into a molecular cloud. The CO molecule also exhibits self-shielding (van Dishoeck & Black 1988), but the abundance of CO is ~ 4 orders of magnitude lower than that of H_2. As a result, the column depth at which self-shielding occurs for CO is larger than that for H_2.

In order to estimate the expected distribution of H_2 and CO in a translucent cloud, the chemistry must be modeled numerically. The simplest model of a molecular cloud is that of a homogeneous, isothermal slab of gas with an FUV radiation field incident on one side (e.g., see the work of Tielens & Hollenbach 1985; van Dishoeck & Black 1988; Hollenbach, Takahashi, & Tielens 1991). Following van Dishoeck & Black (1988), a translucent cloud was modeled here as a one-dimensional homogeneous slab. The gas volume density was taken to be $n = 1000\,\mathrm{cm}^{-3}$ and the FUV flux was taken to be the mean interstellar radiation field, $1.6 \times 10^{-3}\,\mathrm{ergs\,cm^{-2}\,s^{-1}}$ (Habing 1968). These are the average physical conditions in translucent high-latitude clouds (van Dishoeck *et al.* 1991). The temperature of the cloud as a function of visual extinction A_v was computed using the analytical approximation of Hollenbach *et al.* (1991). This approximation takes into account the gas cooling due to [C II] line emission and gas heating due to photoelectric emission from dust grains. The formation of H_2 occurs primarily on the surface of dust grains, and is relatively simple to calculate. The formation of CO, however, requires a complex network of chemical reactions, the most important of which are shown in Figure 3. The self-shielding of H_2 and CO, and the shielding of CO by H_2 (Tielens & Hollenbach 1985; van Dishoeck & Black 1988) were taken into account in this model.

The steady-state abundances of 27 chemical species containing H, He, C, and O, which undergo 134 gas-phase reactions, were calculated numerically. The calculated concentrations of H_2 and the three most abundant forms of carbon—carbon monoxide (CO), neutral atomic carbon (C I), and singly-ionized carbon (C II)—are plotted as a

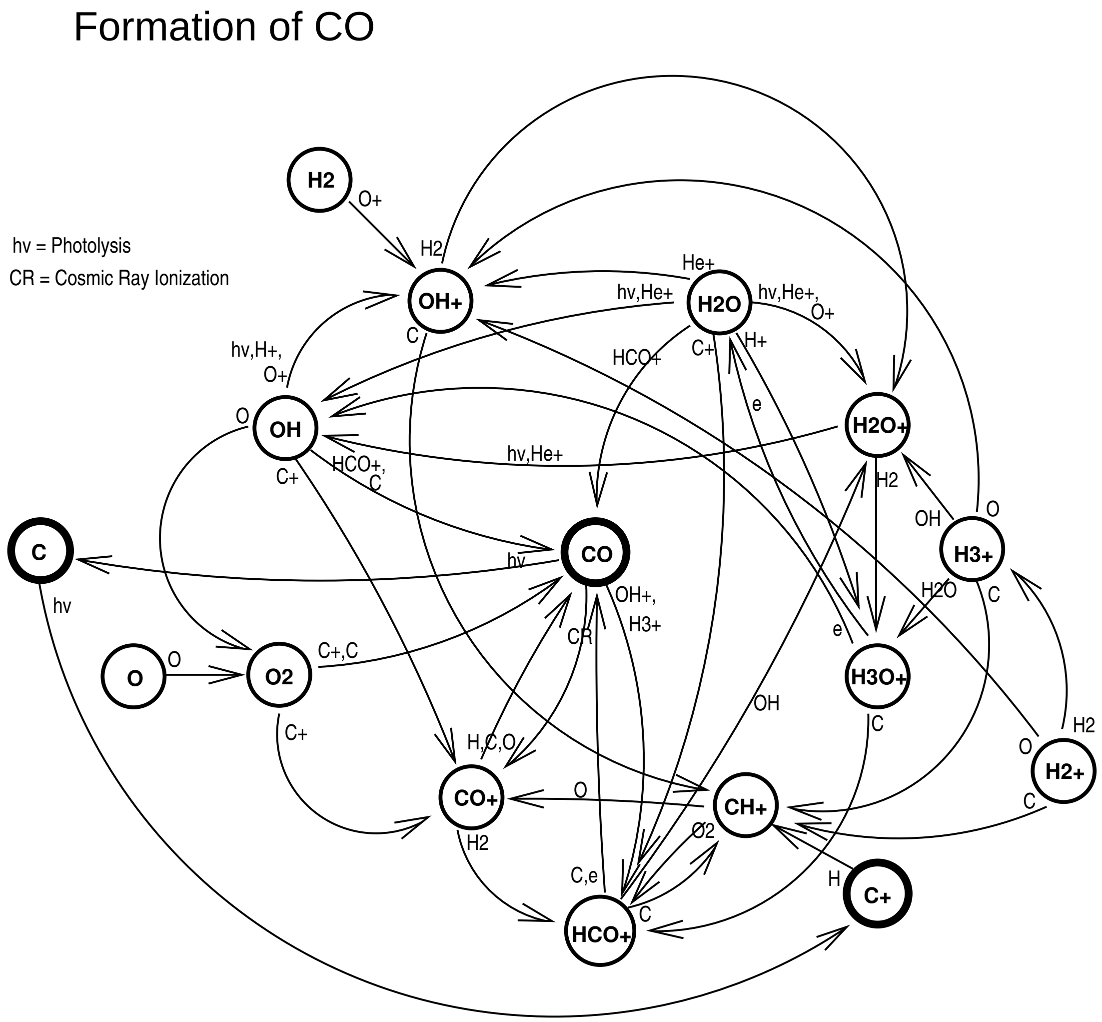

Fig. 1.3.— The CO formation network used in the model shown in Figure 4.

function of $\mathrm{A_v}$ in Figure 4 (Top). The bottom panel of Figure 4 is a plot of the more observationally relevant quantity, the species column density. The column density of species i, N_i, may be derived from the computed volume density, n_i:

$$N_i(\mathrm{A_v}) = 2.5 \times 10^{21} (\,\mathrm{cm}^{-2}/\mathrm{mag})\;\; \frac{\int_0^{\mathrm{A_v}}\; n_i(\mathrm{A_v}')\, dA_v'}{n}. \tag{1.1}$$

Here the conversion between visual extinction, $\mathrm{A_v}$, and total gas column density, $\mathrm{N_H}$,

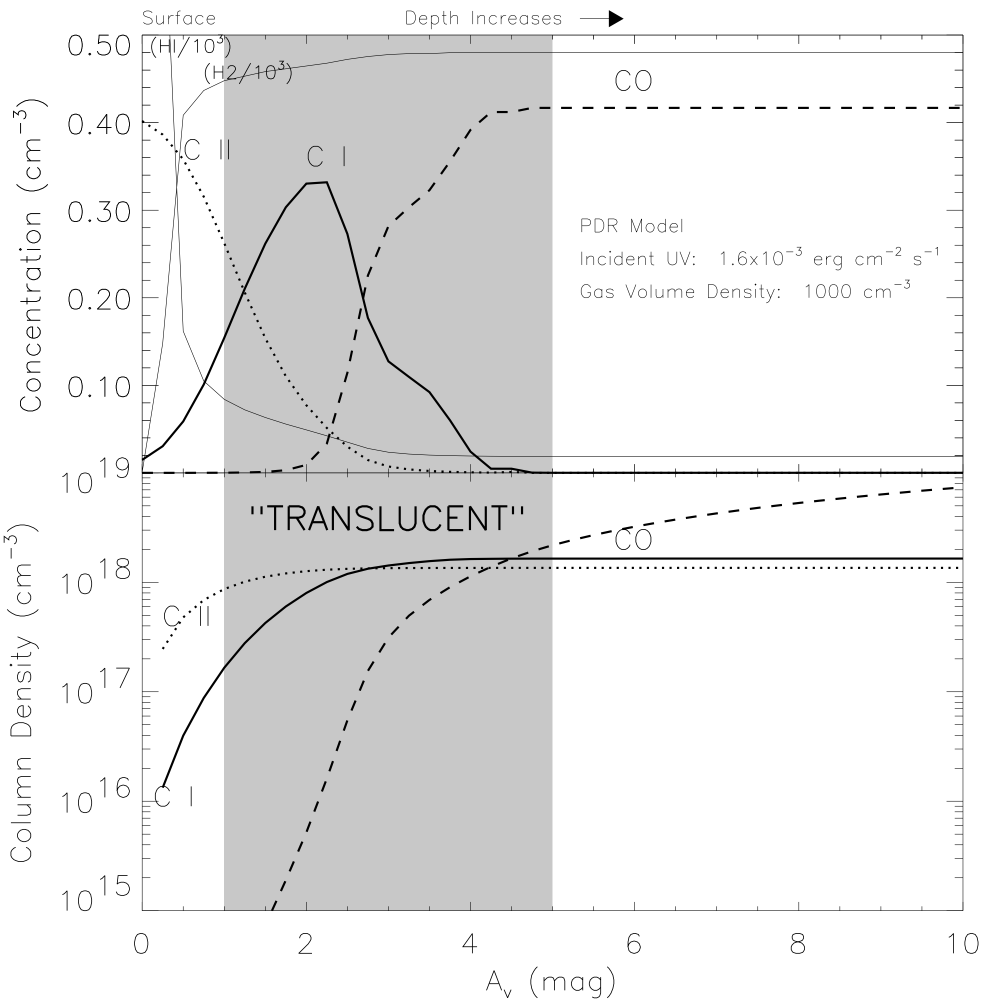

Fig. 1.4.— Steady-state PDR calculation for carbon gas in a translucent cloud. The concentrations (top) and column densities (bottom) of CO, C I, and C II are plotted as a function of visual extinction A_v for a homogeneous cloud with density $n = 1000\,\mathrm{cm}^{-3}$. Here a plane–parallel cloud is illuminated at its edge by the mean interstellar radiation field (ISRF). The gas temperature as a function of A_v was computed using the analytical formula of Hollenbach *et al.* (1991). The translucent regime is indicated by the shaded region. The thin solid lines in the top frame indicate the concentration of H I and H_2, divided by 1000.

recommended by Gordon (1995) is used:

$$N_{\mathrm{H}} \;=\; 2.5\times10^{21}(\,\mathrm{cm}^{-2}/\mathrm{mag})\;\; A_{\mathrm{v}}. \tag{1.2}$$

The structure of a plane-parallel slab exposed to the interstellar radiation field is shown in Figure 4. At $A_v \sim 0.5\,$mag, corresponding to a hydrogen column density of $\sim 2\times10^{20}\,\mathrm{cm}^{-2}$, H_2 becomes the most abundant species, in agreement with Federman *et al.* (1978). At this value of A_v, the carbon is mostly in ionized form. By $A_v \sim 1\,$mag, C I becomes the most abundant carbon species. It is not until $A_v \sim 3\,$mag, however, that CO dominates the other carbon species.

The shaded region in Figure 4 shows the range in A_v for which a cloud is translucent. The translucent cloud has comparable column densities of carbon in all three forms: CO, C I, and C II. In addition, these species seem to be distributed over regions of comparable size, all of which contain significant amounts of H_2. According to the model, *there are large portions of translucent clouds in which H_2 is the most abundant species, but in which there is little or no CO.* The regions in which C I and C II are the most abundant carbon species are regions in which the CO photodissociation dominates over formation. These regions are called *photodissociation regions*, or PDRs (Tielens & Hollenbach 1985). The concept of a PDR was originally introduced to describe the conditions at the edges of dense molecular clouds directly exposed to the UV radiation from nearby stars. Figure 4 shows that a translucent cloud is in fact an isolated PDR. To understand the structure and distribution of translucent H_2 gas properly, one should not rely solely on measurements of the transitions of CO, but also those of the other carbon-bearing PDR tracers, C I and C II.

1.2 Dissertation Outline

The submillimeter band is a critical one for astronomy.

Phillips & Keene (1992)

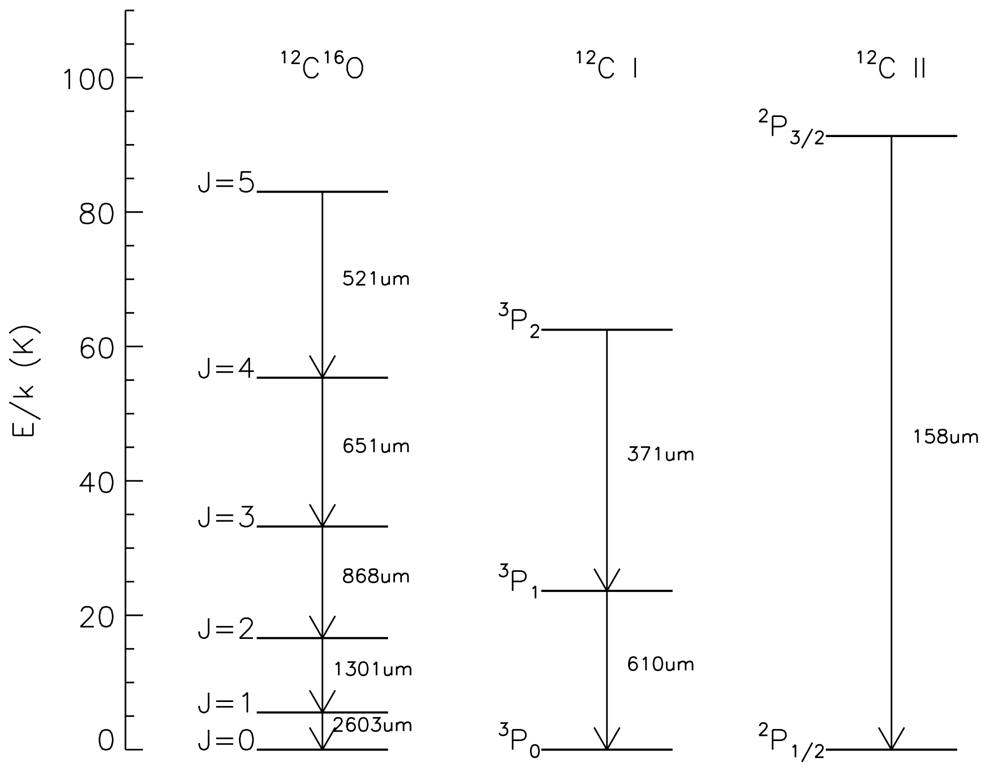

Fig. 1.5.— Energy level diagrams for the lowest transitions of the three most common species of gas phase carbon. (Phillips & Keene 1992)

The main goal of this dissertation is to constrain the structure and distribution of translucent H_2 using observations of the millimeter, submillimeter, and far-infrared emission lines of CO, C I, and C II towards a sample of translucent HLCs. An attempt will be made to answer the following question. How are CO, C I, and C II distributed in translucent HLCs, and what is the relationship of these species to H_2?

The lowest-lying energy levels of these most abundant carbon species are shown schematically in Figure 5. Observations of some of the transitions between these levels will be used to address this question, and to test the predictions of translucent cloud models (*cf.*, Figure 4). Particular attention will be given to the problem of how much translucent H_2 is traced by C II and C I instead of CO.

This dissertation relies on the latest advances in submillimeter technology, as well as on the exploitation of two new observatory sites: the South Pole, and the orbiting ISO satellite. Prior to 1993 the HLCs were observed in emission mainly in the millimeter wave CO (J = 1–0) and (J = 2–1) transitions. With the advent of new submillimeter receivers (e.g., Walker *et al.* 1992) the lowest lying [C I] ($^3P_1 \rightarrow {}^3P_0$) transition was observed for the first time towards two translucent HLCs (Ingalls, Bania, & Jackson 1994 (Chapter 6); Stark & van Dishoeck 1994). The installation of the Antarctic Submillimeter Telescope and Remote Observatory (AST/RO; see Chapter 2) at the South Pole opened a new window on the submillimeter sky, and eight new HLCs were detected in [C I] emission (Ingalls *et al.* 1997; Chapter 4). The launch of the Infrared Space Observatory in 1995 resulted in the first detections of the [C II] ($^2P_{3/2} \rightarrow {}^2P_{1/2}$) transition towards HLCs. Some of those detections will be shown in Chapter 5.

The dissertation consists of three major parts. Part 1 (Chapters 1, 2, and 3) is a general introduction to the scientific problem to be investigated, and the techniques with which it will be investigated. Part 2 (Chapters 4 and 5) is a general study of CO, C I, and C II in southern HLCs. Part 3 (Chapters 6 and 7) will describe the application of the results of Part 2 to a specific HLC, MBM-12, and will discuss the astrophysical implications of the results.

In the first part, Chapter 1 (the current chapter) introduces the problem of how to probe H_2 in the translucent interstellar medium. It is suggested that only by using observations of all three carbon species, CO, C I, and C II, can the conditions in the H_2 gas be understood. Chapter 2 introduces the newest submillimeter instrument, the Antarctic Submillimeter Telescope and Remote Observatory (AST/RO). The chapter also describes the effects of atmospheric water vapor on submillimeter astronomical signals, and investigates the long-term stability of the submillimeter sky at the South Pole and Mauna Kea. The sample of translucent high–latitude clouds studied here is introduced in Chapter 3.

In the second part, Chapter 4 describes a study of the overall CO and C I properties of southern hemisphere HLCs made with the AST/RO telescope. The physical conditions in the CO and C I gas are inferred by using three rotational transitions of CO, as well as *IRAS* dust continuum images. Chapter 5 discusses Infrared Space Observatory (ISO) observations of C II and far-infrared continuum emission towards four HLCs. The physical conditions in the C II gas are inferred from the line intensities, and the results are compared with *COBE* all-sky observations.

In Chapter 6, the results of Chapters 4 and 5 are applied to high resolution CO and C I observations of the prototype HLC, cloud MBM-12, made using the Caltech Submillimeter Observatory. Here the structure of the molecular gas is further constrained, and models of translucent cloud chemistry are tested. Chapter 7 summarizes the work and places the results of Chapters 4, 5, and 6 in the general context of molecular cloud astrophysics.